Int. J. Multiphase Flow Vol. 16, No. 1, pp. 1–17, 1990
Printed in Great Britain.

0301-9322/90 $3.00 + 0.00

MONTE CARLO SIMULATION OF GAS–SOLIDS SUSPENSION FLOWS IN IMPINGING STREAMS REACTORS

A KITRON,[1] T. ELPERIN[2,3] and A. TAMIR[1]

Departments of [1]Chemical and [2]Mechanical Engineering and [3]Pearlstone Center for Aeronautical Engineering Studies, Ben-Gurion University of the Negev, Beer-Sheva 84120, Israel

(*Received* 23 *November* 1988; *in revised form* 29 *May* 1989)

Abstract—Impinging streams reactors have been employed in various fields of chemical engineering, as a means of enhancing the rates of convective transfer processes. The analysis of the hydrodynamics of gas–solids suspension flows in these reactors requires that collisions between particles be taken into account. The stochastic model for gas–solids suspension flows, based on the Boltzmann transport equation, is presented. The system of nonlinear integro-differential transport equations is solved using the Monte Carlo method. A qualitative agreement is obtained between the predicted and experimental results for the particle concentration distribution in an impinging streams reactor. The particle concentrations in the impingement zone of two particle-laden jets are strongly reduced by the effects of inter-particle collisions. The analysis of laminar pipe flows in the absence of gravity and lift forces (Saffman force etc.) reveals a collision-induced migration of particles towards the pipe wall and, to a lesser extent, towards the core. In turbulent vertical pipe flow, particles migrate towards the pipe core and the laminar sublayer. Collison-induced effects become more pronounced in mixture flows with particles of different sizes and densities.

Key Words: impinging streams, two-phase flows, Boltzmann equation, Monte Carlo method

1. INTRODUCTION

Fluidized or spouted beds of granular materials (e.g. Perry & Chilton 1973, Chap. 20, pp. 16–74) are commonly used in processes involving gas–solid particles suspensions. The rate of convective transfer processes, such as drying, leaching, combustion and mixing of particles, is an increasing function of the relative velocity between the phases. In such apparatus, however, the relative velocity between the phases cannot exceed the fluidization velocity, which is relatively small. In order to compensate for the low transfer rates, longer particle residence times are required, necessitating larger equipment volumes or longer batch durations.

Impinging streams reactors, first proposed by Elperin (1961), have been suggested as an alternative method. In such reactors, two gas–solids suspension streams flowing in opposite directions are allowed to impinge (see figure 1). Assuming that the solid particles are initially at kinematic equilibrium, i.e. moving with a velocity identical to that of the gas, and that particles maintain high relative velocities when penetrating the opposite stream, the relative velocity between the phases reaches up to twice the gas inlet velocity. After penetrating into the opposite stream, particles attain a kinematic equilibrium with the gas, are carried into the original stream and so forth. These particle oscillations between the streams result in increased particle residence times. The merits of impinging streams reactors have recently resulted in their employment for various chemical engineering applications. However, inter-particle collisions apparently decrease the particle residence time in the system, thereby impairing the reactor's performance (Elperin 1972; Tamir & Kitron 1987).

While impinging streams reactors constitute a new motivation for modelling particle collisions in suspension flows, inter-particle collisions have long hindered the analysis of industrial systems such as pneumatic transport of solids, fluidized beds etc. In addition to averaged flow behaviour, the statistical distribution of the particle flow properties deserves attention as a potential aid for facilitating the cumbersome measurement of dispersed-phase properties in multiphase flows (e.g. Hetsroni 1982, Chap. 10, pp. 113–118). The aim of this work is to investigate collision-induced phenomena in gas–solids suspensions using the stochastic model based on the Boltzmann transport equation and the Monte Carlo method.

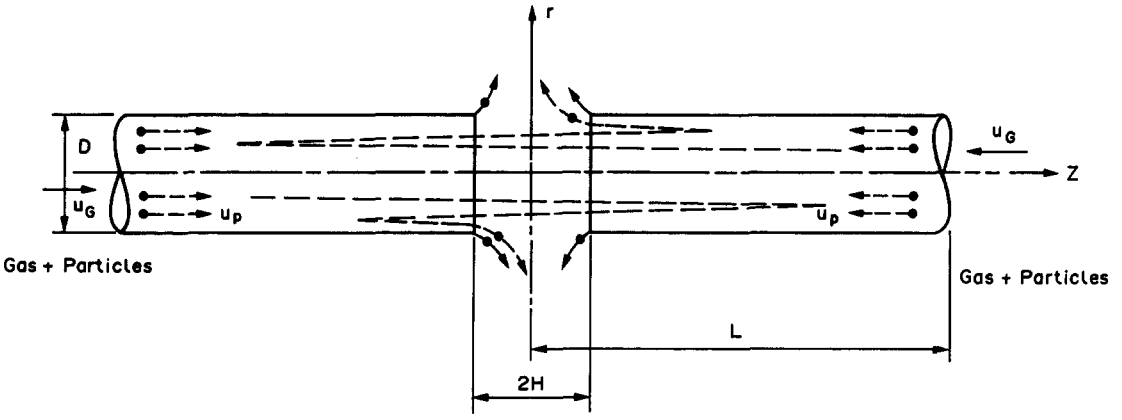

Figure 1. Scheme of an impinging streams reactor.

Collisions between particles are caused by differences in particle velocities. The collisions arise due to differences in the response to a flow field by particles of different size or mass, flow field shear, stochastic effects in the flow field, such as fluid turbulence and Brownian motion, and random excitations of the flow field such as wakes, sonic waves and flow instabilities.

An analogy between particle collisions in suspensions and molecular collisions encountered in the kinetic theory of gases enables the application of the Boltzmann equation for the solid particles, as first suggested by Culick (1964) and Pai (1974). Effects which must be accounted for in the derivation of the Boltzmann equation for suspension flows, and which are normally insignificant in the derivation of the Boltzmann equation in gas dynamics, include solid particle–gas interactions, involving velocity-dependent forces, inelasticity and friction in particle collisions and a size distribution among the particles. An advantage of the statistical mechanics approach in suspension flow modelling is the availability of experimental data about the dynamics of inter-particle collisions.

Consider the flow of a gas carrying small spherical irrotational solid particles of different sizes. The suspension is considered to be sufficiently dilute for the particle motion to be described as collisionless motion due to forces exerted by the gas, interrupted by inter-particle collisions. Only binary collisions between particles are considered, and the duration of a collision is assumed to be negligibly small compared to the time of collisionless motion. The latter assumption allows us to neglect hydrodynamical effects during collisions, and is valid when the ratio of the solid particle density ρ_p to the gas density ρ_G is much greater than unity, i.e. $\rho_p/\rho_G \gg 1$ (Marble 1964). Furthermore, inter-particle collisions are assumed to only involve pairs of particles having uncorrelated pre-collision velocities. The above assumptions are similar to those made in the derivation of the Boltzmann transport equation in gas dynamics (e.g. Lifshitz & Pitaevskii 1981, pp. 67–72).

In order to apply the above model, the deviation in the trajectories of colliding particles due to hydrodynamical interaction, causing a reduction in collision rate (Langmuir & Blodget 1948; Michael & Norey 1969), must be neglected. The validity of this assumption is discussed below.

The dynamics of inter-particle collisions have been considered in detail by Jenkins & Savage (1983), Ogawa (1983) and Soo (1983). Supposing the outward unit normal vector $\mathbf{n}$ at the collision surface to be constant during particle collisions, particle velocities normal to the plane of contact before and after the collision are related by the following empirical expression:

$$(\mathbf{v}_1' - \mathbf{v}_2')\cdot\mathbf{n} = -\epsilon(\mathbf{v}_1 - \mathbf{v}_2)\cdot\mathbf{n}, \qquad [1]$$

where $\mathbf{v}$ is a linear velocity, 1 and 2 are particle indices, primes denote post-collision values and ϵ ($0 < \epsilon < 1$) is the restitution coefficient. The case of $\epsilon = 1$ corresponds to an elastic collision. The friction between colliding particles causes a reduction in the relative velocity in the direction tangential to the plane of collision:

$$(\mathbf{v}_1 - \mathbf{v}_2)\cdot\boldsymbol{\tau} - (\mathbf{v}_1' - \mathbf{v}_2')\cdot\boldsymbol{\tau} = \eta(1+\epsilon)(\mathbf{v}_1 - \mathbf{v}_2)\cdot\mathbf{n}, \qquad [2]$$

where η is the coefficient of solid friction and $\boldsymbol{\tau}$ is a unit vector normal to the vector $\mathbf{n}$.

According to these assumptions, a collision between two particles of masses m_α, α being the particle index, results in the following particle linear velocities:

$$\mathbf{v}'_\alpha = \mathbf{v}_\alpha + (-1)^\alpha\left(\frac{\mu}{m_\alpha}\right)\{(1+\epsilon)[(\mathbf{v}_1-\mathbf{v}_2)\cdot\mathbf{n}]\mathbf{n} + (1-R)[(\mathbf{v}_1-\mathbf{v}_2)\cdot\boldsymbol{\tau}]\boldsymbol{\tau}\}, \quad [3]$$

where μ is the reduced mass, given as

$$\mu = \frac{m_1 m_2}{(m_1+m_2)}; \quad [4]$$

and R is given as

$$R(\theta) = \begin{cases} 1-\eta(1+\epsilon)\operatorname{cotan}\theta & \text{if } \theta^* \leqslant \theta \leqslant \dfrac{\pi}{2} \\ 1 & \text{if } 0 \leqslant \theta \leqslant \theta^*, \end{cases} \quad [5]$$

where

$$\theta = \cos^{-1}\left(\frac{\mathbf{n}\cdot(\mathbf{v}_1-\mathbf{v}_2)}{|\mathbf{v}_1-\mathbf{v}_2|}\right) \quad [6]$$

and

$$\theta^* = \tan^{-1}\eta(1+\epsilon). \quad [7]$$

The discontinuity in R arises from the stipulation that friction does not reverse the relative velocity between the particles.

Applying this collision dynamics model and the assumptions listed above, the Boltzmann equation for the particle distribution function in a mixture of particles of s types may be derived following the standard procedure (e.g. Lifshitz & Pitaevsky 1981, pp. 7–11), yielding a set of coupled transport equations:

$$\begin{aligned} &\frac{\partial f_i(\mathbf{v},\mathbf{v},t)}{\partial t} + \nabla_{\mathbf{r}}\cdot[\mathbf{v}f_i(\mathbf{v},\mathbf{r},t)] + \nabla_{\mathbf{v}}\cdot\left[\frac{\mathbf{F}f_i(\mathbf{v},\mathbf{r},t)}{m_i}\right] \\ &\quad = S_i(\mathbf{v},\mathbf{r},t) + \sum_{j=1}^{s}\int_{W_{\mathbf{v}}}\int_0^{4\pi}[(\epsilon J)f_j(\mathbf{v}',\mathbf{r},t)f_i(\mathbf{v}'_1,\mathbf{r},t) \\ &\qquad - f_j(\mathbf{v},\mathbf{r},t)f_i(\mathbf{v}_1,\mathbf{r},t)][(\mathbf{v}-\mathbf{v}_1)\cdot\mathbf{n}]\cdot\sigma_{ij}\,d\mathbf{v}_1\,d\Omega \\ &\quad = S_i(\mathbf{v},\mathbf{r},t) + I_i(f,f), \end{aligned} \quad [8]$$

where $f_i = f_i(\mathbf{v},\mathbf{r},t)$ is the distribution function for particles of type i; $\mathbf{r}$ is a position vector; t is the time; $\mathbf{F}/m$ is the particle acceleration due to body forces and gas friction; $S_i(\mathbf{v},\mathbf{r},t)$ is the external source term for particles of type i; the velocities $\mathbf{v}'$ and $\mathbf{v}'_1$ are related to $\mathbf{v}$ and $\mathbf{v}_1$ by [3]; σ_{ij} is the collision cross-section, given as $\pi(d_i+d_j)^2/4$ for a collision between particles of diameters d_i and d_j; $d\Omega$ is the differential solid angle; and $W_{\mathbf{v}}$ is the domain in the space of velocities. The (ϵJ) factor, appearing in the collision term, arises from the above-mentioned inelasticity and friction in particle collisions, with J being the Jacobian of the transformation $(\mathbf{v}_i,\mathbf{v}_j)\rightarrow(\mathbf{v}'_i,\mathbf{v}'_j)$:

$$J = \frac{d\mathbf{v}'_i\,d\mathbf{v}'_j}{(d\mathbf{v}_i\,d\mathbf{v}_j)}. \quad [9]$$

Ogawa (1983) eliminated the discontinuity in R by averaging it over θ, obtaining, for uniform size particles,

$$J = \epsilon R^2. \quad [10]$$

In the case of elastic, frictionless collisions, $J=1$. The terms appearing on the l.h.s. of the Boltzmann equation describe the convective variations in $f_i(\mathbf{v},\mathbf{r},t)$ along the particle trajectories, while the $I_i(f,f)$ term describes the variation of the distribution function due to binary collisions between particles and the $S_i(\mathbf{v},\mathbf{r},t)$ term accounts for external particle sources or sinks.

Since the above set of nonlinear integro-differential transport equations is as yet beyond analytical solution, numerical methods must be employed. Although the Boltzmann kinetic equation and Monte Carlo simulation methods have been extensively used to solve various rarefied gas dynamics problems, only a few attempts have been made to apply these methods to suspension flows.

Shahinpoor & Ahmadi (1983) employed the Bhatnagar–Gross–Krook approximation for the collision term in the Boltzmann equation to investigate the flow of uniformly sized granular material without gas drag effects. The kinetic equation was solved by the Chapman–Enskog method to obtain expressions for the stress tensor and the flux vector of the random fluctuation energy in the granular material. Based on these expressions, a complete set of conservation equations was derived and solutions were obtained for granular material gravity flow over an inclined plane and for Couette flow.

Jenkins & Savage (1983) have developed a simple kinetic theory for the rapid flow of identical, smooth, nearly elastic particles. Under the assumption that the distribution function is locally Maxwellian, they derived the first hydrodynamic approximation of the Boltzmann equation. The application of the obtained conservation equations to the shear flow of granular material between two moving plates yielded solutions in quantitative agreement with experimental data. However, this approach cannot resolve the difficulties associated with the formulation of boundary conditions and with the extension of the theory to account for dynamic interactions with the surrounding gas.

Haff (1983) has applied a kinetic theory to determine transport coefficients for granular media. Although the approach applied was entirely heuristic, it provides a very penetrating analysis of kinetic effects in granular material flows.

In another application to granular material flow, Ogawa (1983) employed the Monte Carlo method to find a solution of the Boltzmann equation for a spatially homogeneous flow of rotating particles of equal size, without external forces and gas drag, obtaining the distribution of the particle kinetic and rotational energy as a function of time.

Pearson *et al.* (1984) applied the Monte Carlo method to describe the agglomeration of minute particles which take up the gas velocity instantly. Assuming space-homogeneity of all properties and letting particles adhere to each other upon contact, they calculated the evolution of the particle size distribution in laminar and turbulent flows.

This work provides a method for the Monte Carlo simulation of a gas–solids suspension flow described by the above system of transport equations, taking into account gas friction effects, spatial nonhomogeneity and the size distribution among particles. Solutions are presented for pipe flows and impinging streams, pertaining to impinging streams reactors.

2. EMPLOYMENT OF THE MONTE CARLO DIRECT SIMULATION METHOD

2.1. Background

In this work, the direct simulation Monte Carlo (DSMC) method, first suggested by Bird (1976) for solving the Boltzmann equation appropriate to rarefied gas dynamics, is adapted for simulating solid particle flow in a gaseous suspension.

The key ideas of the DSMC method devised by Bird are: (a) the uncoupling of free molecular motion during a time step Δt_m from collisions, i.e. the use of the operator-splitting technique; (b) the simulation of molecular collisions by disregarding molecular positions within spatial cells; and (c) the simulation of fewer particles than those in the real flow, while normalizing the collision cross-section so that the collision rate is not changed. Assumption (a) is valid when Δt_m is smaller than the time between collisions and larger than the collision duration, and assumption (b) is valid provided that the cells are so small that the spatial variation of flow variables in the cell is negligible.

The following is an outline of the operator-splitting technique in Bird's method. Let $f_i^n(\mathbf{r}, \mathbf{v})$ approximate the distribution function at the nth time step, i.e. at time $t = n \cdot \Delta t_m$. To obtain the solution $f_i^{n+1}(\mathbf{r}, \mathbf{v})$ at the $(n+1)$th time step, we consider first the collisionless transport equation

$$\frac{\partial \Phi_i}{\partial t} + \nabla_{\mathbf{r}}(\mathbf{v}\Phi_i) + \nabla_{\mathbf{v}}\left(\frac{\mathbf{F}\Phi_i}{m}\right) = S_i(\mathbf{r}, \mathbf{v}, t), \qquad [11]$$

with $f_i^n(\mathbf{r}, \mathbf{v})$ accepted as the initial value. At the second stage, $f_i^{n+1}(\mathbf{r}, \mathbf{v})$ is obtained by solving the homogeneous Boltzmann equation

$$\frac{\partial f_i^{n+1}}{\partial t} = I_i(f^{n+1}, f^{n+1}), \qquad [12]$$

with the solution Φ_i obtained at the first stage as the initial value. The solution of this equation at time $(n+1)\,\Delta t_m$ is found by sampling binary collisions between particles, as described below. The overall solution is thus accurate to the first order in both time and spatial increments.

It is worth noting that properly setting the boundary conditions for the Boltzmann transport equations is rather difficult. A very important advantage of the Monte Carlo method is its suitability for treating boundary conditions in a natural, simple manner, as described below.

2.2. Simulation algorithm

Under the assumptions listed in the above formulation of the system of coupled transport equations, and employing Bird's assumptions (a) and (b) mentioned above, the DSMC method for the flow of a gas–solids suspension is described as follows. The flow system is divided into equal-volume cells. Simulated particles are distributed in the system, with their positions and velocities sampled from the initial distribution function. When a stationary system of transport equations is solved, the initial distribution function is chosen arbitrarily, and the stationary solution is obtained by relaxation techniques, i.e. as the long-time asymptotics of the nonstationary solution. Particles are allowed to move in the system, without colliding with each other, for a time interval Δt_m, with their subsequent positions and velocities determined from the particle's equation of motion. Within the time interval Δt_m, a particle may encounter a boundary: either an open boundary, where particles exit from the system; or a wall, where the particle's velocity after the collision (taken to be negligibly short) is calculated according to the model adopted for the collision's dynamics, i.e. the elasticity and friction.

Following the collisionless motion, particles are allowed to collide with each other. Let $N_{m,k}$ be the number of particles of type k in cell m having a volume V_m. The total number of particles in cell m is

$$N_m = \sum_{k=1}^{s} N_{m,k}. \qquad [13]$$

A pair of colliding particles of types i and j is sampled from the N_m particles with probability $\sigma_{ij} v_{ij}/(\sigma_{ij}^* v_{ij}^*)$, where v_{ij} is the relative velocity between the particles and v_{ij}^* and σ_{ij}^* are the maximal relative velocity and collision cross-section between particles of types i and j in the cell. Particle velocities after collision are calculated from [3]; the normal unit vector $\mathbf{n}$ at the collision surface is assumed to be distributed isotropically. After the collision, a time increment

$$\Delta t_{ij} = \frac{2V_m}{[N_{m,i} N_{m,j} v_{ij} \sigma_{ij}]} \qquad [14]$$

is added to a time counter T_{ij}^m for the collisions between particles of types i and j, in cell m. The combination of particle types having the smallest value of the local time counter T_{ij}^m is chosen for the next collision (Bird 1968); if all T_{ij}^m values are zero, the combination is randomly sampled. This procedure is repeated until all T_{ij}^m values exceed the value $(n+1)\,\Delta t_m$.

The expected number of collisions in cell m during a time interval Δt_m between particles of types i and j is given as

$$\psi_{ij}^m = N_{m,i} N_{m,j} v_{ij} \Delta t_m \frac{\sigma_{ij}}{(2V_m)} = \alpha_{ij} \Delta t_m, \qquad [15]$$

where v_{ij} is the mean relative velocity between particles of classes i and j. The performance of the procedure depends upon the choice of cell dimensions and the value of the time increment Δt_m.

2.3. Choice of particle properties

Consider a dilute suspension of identical spherical particles. The mean spacing between such

particles, when uniformly distributed in space, is given as

$$\delta = \left(\frac{\pi}{6\beta}\right)^{1/3} d, \qquad [16]$$

where β is the average volume fraction of the particles in the system. An average mean-free-path between collisions can be estimated by elementary kinetic theory as

$$\lambda = \left(2^{1/2}\sigma \cdot \frac{6\beta}{\pi d^3}\right)^{-1} = \frac{d}{(2^{1/2} \cdot 6\beta)}. \qquad [17]$$

The upper limit for the particle volume fraction β_{max} is given by the requirement that the mean-free-path between particle interactions be greater than the mean inter-particle spacing δ (Soo 1976). Using the condition $\lambda = \delta$ and [16] and [17] yield $\beta_{max} = 0.055$. However, a more restrictive requirement on β is implied by the assumption that the suspension is sufficiently dilute that only binary inter-particle collisions need be considered.

Clearly, the statistical description of the flow of solid particles is valid only when the number of particles in a unit volume is sufficiently large [see also Haff (1983)]. In the flow systems considered in this work, the solid particle volume fractions are of the order of 0.001, which, for particles of dia $d = 1$ mm, corresponds to particle number densities of the order of $\sim 10^6$ particles/m^3.

In the formulation of the transport equation [8], the deviation in trajectories of approaching particles due to hydrodynamic forces was neglected. This deviation causes a reduction in the particle collision rate by a factor known as the "fraction impacted" or the collision efficiency. For spherical particles of diameter d_s moving with a gas at speed U and colliding with larger particles of diameter d_l, the "fraction impacted" may be neglected [according to data in Soo (1967, p. 193)] when the distance travelled by the smaller particles during the Stokes relaxation time is considerably larger than the diameter of the large particle:

$$\frac{\rho_p U d_s^2}{(18\mu_G d_l)} > 100, \qquad [18]$$

where μ_G is the gas viscosity. For solid particles flowing in a gas, the small gas viscosities and the high particle densities relative to the gas render this effect negligible, unless particle size or velocity are very small.

In order to examine the validity of neglecting the collision duration, consider the expression provided by Soo (1983) for the duration of a collision between two identical spheres:

$$\Delta t_{col} = 2.94 v_{12}^{-1/5} \cos\theta^{-3/5} d\left[5(1+\varepsilon)\frac{\rho_p(1-\nu_p^2)}{16E}\right]^{2/5}, \qquad [19]$$

where ν_P is the particle's Poisson ratio, ρ_p—its density and E—its Young's modulus, and the hydrodynamical relaxation time for Stoke's law is

$$\tau_h = \frac{\rho_p d^2}{(18\mu_G)}. \qquad [20]$$

According to [15] and [16], the collision frequency for a single particle of type i is given as

$$\nu_i = \sum_{j=1}^{s} \frac{\pi(d_i + d_j)^2 v_{ij}\left(\frac{6\beta}{\pi d^3}\right)}{4}. \qquad [21]$$

For characteristic values of $d = 0.001$ m, $\rho_p = 1000$ kg/m^3, $\beta = 0.01$, $\mu_{air} = 1.75 \times 10^{-5}$ kg/m s, $\varepsilon = 0.8$, $\theta = 45°$, $v_{12} = 0.1$ m/s, $\nu_P = 0.4$ and $E = 5 \times 10^9$ Pa, one obtains $\Delta t_{col} = 8.9 \times 10^{-6}$ s, $\tau_h = 0.18$ s and $1/\nu = 6$ s (for $\theta = 89.99°$, one obtains $\Delta t_{col} = 1.3 \times 10^{-3}$ s). Thus, the collision duration can be neglected.

A certain restriction may arise concerning the relation between the hydrodynamical relaxation time, τ_h, and the mean time between collisions, $1/\nu$. The assumption that colliding particles have uncorrelated velocities, necessary for the derivation of the transport equation [8], is valid for gas dynamics due to the high rate of collisions between molecules (in addition to the high particle number densities). Since suspension flow involves a much smaller inter-particle collision rate than

the molecule collision rate in gas flow, the hydrodynamical dampening of post-collision velocities should be strong enough to prevent such a correlation. If the hydrodynamical relaxation occurs too quickly, particles have small relative velocities in relation to the gas, so that their velocities are highly correlated with respect to the gas velocity at the location of the collision.

The latter conclusion is equivalent to the requirement that the particle self-collision Knudsen number $\mathrm{Kn} = \lambda/D = d/(2^{1/2}6\beta D)$, where D is a characteristic macroscopic length, must not considerably exceed the Kn for particle collisions with gas molecules, $\mathrm{S} = \tau_h U/D$, where U is a characteristic flow velocity. Particularly, in cases where $\mathrm{S} \ll \mathrm{Kn}$, the effect of inter-particle collisions is insignificant, since the particles take up the gas velocity instantly.

2.4. Choice of cell dimensions

Bird (1976) set a cell dimension h, in a direction across which the particle concentration and average velocities vary, as $h < \lambda/3$. Still, an upper limit for h, which normally does not arise for gas molecules, is given by the stipulation that h be much greater than d (at least by one order of magnitude) so that calculating collisions only within cells is permissible. A general limitation for h is that it should be small enough that the spatial variation of the flow variables in the cell is negligibly small, while large enough to avoid long calculation times.

2.5. Choice of time increments

Bird (1976, p. 119) suggested taking Δt_m smaller than the mean time between collisions $1/\nu$, so as to validate the uncoupling of the collisions between particles from their collisionless motion. When mixtures of particles of different sizes are considered, Δt_m should be taken smaller than the shortest estimated $1/\nu_i$.

It should be noted that the stability of the explicit two-stage operator-splitting procedure described above (see [11] and [12]) requires that the time increment and cell size satisfy the Courant–Lewy–Friedrichs condition, whereby $\Delta t_m < h/\mathbf{v}^*$, where $\mathbf{v}^*$ is a characteristic particle velocity. This condition is consistent with [17] and [21] for λ and ν and Bird's requirement that $\Delta t_m < 1/\nu$.

2.6. Equation of collisionless particle motion

When only fluid drag acts upon particles during t_m, a particle's trajectory is calculated by integrating the ordinary differential equation

$$\frac{\mathrm{d}^2\mathbf{r}}{\mathrm{d}t^2} = 0.75 C_\mathrm{D}\left[\frac{\rho_\mathrm{G}}{(\rho_\mathrm{p} d)}\right]|\mathbf{U}-\mathbf{v}|(\mathbf{U}-\mathbf{v}) + \boldsymbol{g}, \qquad [22]$$

where $\mathbf{U}$ is the gas velocity at $\mathbf{r}$, $\boldsymbol{g}$ is the gravity acceleration and C_D, the gas drag coefficient for a single spherical particle, is correlated as (Clift *et al.* 1978, p. 112) $C_\mathrm{D} = f(\mathrm{Re}_\mathrm{p})$, where

$$\mathrm{Re}_\mathrm{p} = \frac{\rho_\mathrm{G} d|\mathbf{U}-\mathbf{v}|}{\mu_\mathrm{G}}. \qquad [23]$$

When the gas shear induces a considerable lift on the particles, [22] is modified by taking account of the Saffman (1965) force, acting in the radial direction and having a magnitude

$$F_\mathrm{S} = \frac{1.61\mu_\mathrm{G}^{1/2}\rho_\mathrm{G}^{1/2}(U_z - v_z)d^2\left(\dfrac{\mathrm{d}U_z}{\mathrm{d}r}\right)}{\left|\dfrac{\mathrm{d}U_z}{\mathrm{d}r}\right|^{1/2}}, \qquad [24]$$

where r and z are the radial and axial coordinates, respectively. The Saffman force causes transverse migration of solid particles having smaller axial velocities than that of the gas in the direction of the axial velocity gradient; the direction of the Saffman force is reversed when a particle's axial velocity exceeds that of the gas. Notably, Saffman's (1965) theoretical prediction of the lift force due to shear–slip effects was derived for unbounded ambient fluid flow with uniform shear, with $\mathrm{Re}_\mathrm{p} < 1$. However, experimental results reported by Lee (1982, p. 11) confirmed the validity of [24] for rather general flow patterns. Saffman showed that the lift force induced by particle rotation in the gas shear flow is generally small compared to F_S [see also Lee (1982, p. 11)]. The Saffman

force need not be considered if its ratio with respect to the drag force F_D is sufficiently small (Soo 1967, p. 28), i.e. $F_S/F_D = 2.15[d^2(dU/dr)\rho_G/\mu_G]^{1/2} \ll 1$.

The effect of gravity may be neglected when the velocity which a solid particle can acquire during the hydrodynamical relaxation time τ_h, due to buoyancy and gravity forces, is much smaller than the characteristic velocity in the vertical direction U (Soo 1969):

$$\frac{\left(1 - \frac{\rho_G}{\rho_p}\right)\tau_h g}{U} \ll 1. \qquad [25]$$

In this work, the added mass, Basset history and pressure gradient terms in the solid particle equation of motion are neglected. These terms are of very marginal significance for the flow of relatively large solid particles in a gas [see also Lee & Wiesler (1987) and Soo (1976)]. Brownian motion of particles is also neglected, since this effect is negligible for large solid particles, and in convective flows may also be insignificant for aerosols [see also Boothroyd (1971, p. 15)].

The effect of the particle flow on the flow pattern of the carrier gas is also neglected. This dynamical uncoupling is justified for laminar flows if the particle volume fraction in the system is sufficiently small that the gas flow is not affected significantly, and the wakes caused by particle motion decay rapidly. It must be noted that although the instantaneous relative velocity in the flows studied in this work is rather high, the time-averaged relative velocity is relative small. The estimated time-averaged ratio between the stress exerted on the gas by the solid particles to the gas pressure gradient in the absence of solid particles was low for all flows considered. Moreover, experimental results reported by Soo (1967, p. 169) show that the change in the gas velocity distribution caused by the presence of solid particles is generally small.

3. CASES STUDIED

The following representative cases, all pertaining to elements of impinging streams reactors, are examined with a particular emphasis on calculating particle concentration distributions. Particle rotations are neglected, as their effect in the cases examined is expected to be secondary.

3.1. Laminar flow in a pipe

Gas–solid particles suspension flows in pipes are often encountered in industrial systems. A typical example is the flow in the feed section of an impinging streams reactor (figure 1). Consider first laminar gas flow free of entrance effects. The gas axial velocity profile in a pipe of diameter D is then given by the Poiseuille profile, i.e. $U_z = 2\bar{U}[1 - (2r/D)^2]$, where $\bar{U}$ is the average gas velocity in the pipe. Solid particles entrained by the gas will undergo collisions with the surrounding particles, due to velocity differences between particles located at different radii. Moreover, it has been shown (Voinov & Petrov 1977) that the stationary motion of small solid particles in a potential flow of an ideal fluid is unstable; this instability may be another cause for inter-particle collisions in laminar flows.

For a steady flow, only variations across the radial direction of the pipe are of interest, hence an ensemble of particles is followed, disregarding the axial positions of particles. This procedure can be regarded as limited to a pipe segment with periodic boundary conditions at its ends, i.e. a particle leaving through one side is immediately replaced by another particle at the opposite side, having the same velocity and radial location.

3.2. Turbulent flow in a pipe

Consider next turbulent pipe flow of a suspension. The turbulent pulsations in such flows can induce radial particle motion, even if particles do not collide with each other. Lee (1987) has recently attempted to analyse this problem phenomenologically by considering the interactions between the particles and the turbulent flow field, applying the simple pseudo-Stokes law with modified turbulent velocity. A correlation was provided for the coefficient of the turbulent velocity in terms of the particle size and concentration, the local flow Reynolds number and the ratio between particle and fluid densities. This work aims to provide further insight into this phenomenon by analysing the effects of direct inter-particle collisions.

The generally adopted approximation for the gas velocity distribution in a turbulent pipe flow is

$$U_z = 1.25\bar{U}\left(1-\frac{2r}{D}\right)^{1/7} + u_z' \qquad [26]$$

and

$$U_r = u_r' \qquad [27]$$

where the turbulent pulsation velocities, u_r' and u_z', are zero for $2r/D > 0.8$ and are otherwise assumed to be normally distributed random variables with zero mean and standard deviations

$$\frac{(\overline{u_r'^2})^{0.5}}{\left[\bar{U}\left(\frac{f_F}{2}\right)^{0.5}\right]} = -18.89\left(1-\frac{2r}{D}\right)^4 + 43.51\left(1-\frac{2r}{D}\right)^3 - 33.43\left(1-\frac{2r}{D}\right)^2 + 9.17\left(1-\frac{2r}{D}\right) + 0.35 \qquad [28]$$

and

$$\frac{(\overline{u_z'^2})^{0.5}}{\left[\bar{U}\left(\frac{f_F}{2}\right)^{0.5}\right]} = -3.05\left(1-\frac{2r}{D}\right)^4 + 5.18\left(1-\frac{2r}{D}\right)^3 - 1.54\left(1-\frac{2r}{D}\right)^2 + 1.98\left(1-\frac{2r}{D}\right) + 2.11, \qquad [29]$$

where f_F, the Fanning friction factor for the gas in the pipe, is taken from Perry & Chilton (1973, Chap. 5, p. 22) as a function of wall roughness and the pipe Reynolds number, $\mathrm{Re}_D = D\bar{U}\rho_G/\mu_G$. Expressions [28] and [29] for the root-mean-square values of the fluctuating components of the fluid velocity were obtained by Yoshida & Masuda (1980) using the least-squares method to correlate Laufer's (1954) measurements of turbulent pipe flows.

Turbulent velocity pulsations are assumed constant during the average lifetime of a turbulent eddy, estimated as the Lagrangian time scale of the turbulent gas flow (see Hinze 1975, p. 426):

$$\tau_L = \frac{0.08[(\overline{u_r'})^2 + (\overline{u_z'})^2]}{\varepsilon_t}, \qquad [30]$$

where ε_t is the specific energy dissipation rate. In turbulent pipe flow of a particle-free gas, $\varepsilon_t = 2\bar{U}^3 f_F/D$.

Clearly, this approach would be a rather rough approximation for an inhomogeneous non-stationary turbulent velocity field. Nevertheless, Lawn's (1971) measurements of the turbulent energy dissipation and the spectral distributions of stress components in the core of a turbulent pipe flow strongly suggest that the turbulent velocity field is locally homogeneous and stationary for $\mathrm{Re}_D > 10^5$. Another condition for the validity of the above approach is that the particles should not be affected by the motion of the smallest eddies. The latter requirement is violated when the hydrodynamical relaxation time τ_h is of the same order of magnitude as the characteristic time for the motion of the smallest eddies, $\tau_s = [\mu_G/(\rho_G\varepsilon_t)]^{1/2}$. Then, using [20] for τ_h, the restriction on the particle diameter is

$$d \sim \frac{L_K}{\left(18\frac{\rho_P}{\rho_G}\right)^{1/2}}, \qquad [31]$$

where L_K is the Kolmogorov microscale length, $L_K = [\mu_G^3/(\rho_G^3\varepsilon_t)]^{1/4}$. Therefore, for large values of $\rho_p/\rho_G \sim 1000$, as studied in this work, only particles smaller by two orders of magnitude than the Kolmogorov microscale length may respond to the smallest eddies. For air flow with a characteristic value of $\varepsilon_t = 300$ W/kg, $L_K \sim 0.06$ mm, so that the above restriction is violated only for submicronic particles. For comparison, let us calculate the Lagrangian scale for characteristic flow values of $(\overline{u'^2})^{1/2} = 2$ m/s and $\varepsilon_t = 300$ W/kg, obtaining $L_L = \tau_L(\overline{u'^2})^{1/2} = 2$ mm, which is of the same order of magnitude as the diameters of solid particles studied in this work.

The assumption equivalent to "molecular chaos" in the formulation of the Boltzmann equation requires in the case of turbulent suspension flow that: (i) the turbulent of the suspending fluid be isotropic on the length scale of the collision process; and (ii) particles be projected at each other from independently moving fluid elements. In the stochastic model described above, the above assumption is implied by sampling for different particles' independent gas fluctuation velocities. As discussed by Abrahamson (1975), condition (i) is likely to be met in industrial pipe flows of gases at sufficiently high Reynolds numbers, where the characteristic correlation length of the turbulent velocity field is much smaller than the particle's free path length and diameter. Condition (ii) requires that the particle's hydrodynamical relaxation time τ_h be larger than the Lagrangian time scale τ_L, since τ_L may be regarded as the average time for fresh fluid to surround a large particle, or as an average time for a very small particle to travel the minimal correlation length scale of the turbulent velocity field. Abrahamson (1975) showed that the condition $\tau_h \gg \tau_L$ implies that $d^2 \gg 15\mu_G(u'^2)/(\rho_p \varepsilon_t)$, which is easily met for solid particles $>100\,\mu$m, flowing in a gas, in most industrial systems.

To account for shear-induced lift forces acting upon particles flowing in a turbulent gas, the shear may be approximated by only considering gradients in the average gas velocity.

The modulation of the gas turbulence pattern by the presence of the particles is neglected. Experimental investigations (e.g. Al-Taweel & Landau 1977) have shown that turbulence modulation by 60 mm particles was significant at particle volume fractions as small as 1×10^{-4} m. However, the turbulence modulation may be less significant for larger particles with similar volume fractions. Owen (1969) derived estimates for the change in the turbulence intensity and energy dissipation rate due to the presence of particles in dilute suspensions:

$$\kappa = \left[\frac{\overline{U'^2}(\beta > 0)}{\overline{U'^2}(\beta = 0)}\right]^{1/2} \sim \begin{cases} \left[1 + \dfrac{\beta\rho_p}{\rho_G}\right]^{1/2}, & \tau_h \ll \tau_L \\ \left[1 + \left(\dfrac{\beta\rho_p}{\rho_G}\right)\left(\dfrac{\tau_L}{\tau_h}\right)\right]^{-1/2}, & \tau_h \sim \tau_L \end{cases} \quad [32]$$

and

$$\xi = \frac{\varepsilon_t(\beta > 0)}{\varepsilon_t(\beta = 0)} \sim \left[1 + \frac{\beta\rho_p}{\rho_G}\right]. \quad [33]$$

Clearly, when $\tau_h \gg \tau_L$, the particle motion is not influenced by turbulent flow fluctuations. Expression [32] was obtained by comparing energy production and energy dissipation rates under the assumption that the turbulent length scale is unaffected by the presence of particles. Substituting characteristic values of the flow parameters used in this work ($\beta = 0.001$, $\rho_p/\rho_G = 1000$, $\bar{U} = 7.5$ m/s, $d = 1$ mm, $D = 0.2$ m, $\mathrm{Re}_0 = 500$, $(u'^2)^{1/2} = 1$ m/s), one obtains $\tau_h = 3.8$ s, $\tau_L = 0.01$ s, $\kappa = 0.999$ and $\xi = 2$. Thus, the modulation of the energy dissipation is seen to be significant, whereas the turbulence intensity may be virtually unaffected by the presence of particles.

3.3. Impinging streams zone

The countercurrent flow configuration in impinging streams reactors causes, as a side effect, collisions between particles, especially between those moving in opposite directions. Collisions often result in increased particle radial velocities, hence a decreased residence time in the reaction zone.

Applying expressions obtained from a potential-flow analysis of a gas jet colliding with a wall, the gas velocity profile in the inter-nozzles region (for $|z| < H$ and $r < D/2$) is given as

$$U_z = \frac{-zU_0}{H} \quad [34]$$

and

$$U_r = \frac{rU_0}{(2H)}, \quad [35]$$

where U_0 is the jet's initial uniform axial velocity and H is the distance from the jet's entrance point

to the wall (plane of impingement, in our case). Elperin (1972) employed this model to perform a qualitative analysis of collision effects in an impinging streams reactor. It is noted that this velocity distribution is not valid at the exit from the feed pipes. As an approximation, a discontinuous gas velocity profile may be applied, with [34] and [35] used in the inter-nozzles region (for $|z| < H$ and $r < D/2$), and $U_z = -zU_0/|z|$ and $U_r = 0$ for all $|z| \geqslant H$ and $r < D/2$.

In the Monte Carlo simulation, following each time interval Δt_m, a quantity of $3\Delta t_m \beta U_0 D^2/(2d^3)$ particles is added into the control volume, in accordance with the gas and particle flow rates. In order to simulate continuous particles feed, to each injected particle is assigned an initial axial location calculated by integrating the particle's equation of motion [22] during a uniformly distributed random fraction of t_m, with initial conditions $v(t=0) = v_0$ and $z(t=0) = L$ (or $L = -L$). Each particle's initial radial location is sampled from a two-dimensional uniform distribution. The initial particle axial velocity v_0 is determined as a fraction of the jet inlet velocity, U_0. The value of v_0 depends upon the length of the channel where particles are accelerated before entering the reactor, so that the lack of kinematic equilibrium between the particles and the carrier gas can be taken into account. In the region $-H < Z < H$ (see figure 1), particles exit from the reactor upon crossing a cylindrical surface of radius $D/2$. Particles reaching the plane $z = L$ or $z = -L$ are specularly reflected back into the simulated control volume.

When the particle flow rates in both streams are equal, the symmetry with respect to the impingement plane is exploited by simulating the particle motion on one side of the control volume, with the plane of symmetry taken to be a specularly reflecting wall.

The Saffman force may be neglected in this case, since the gas velocity in the feed pipes is assumed uniform, and the radial drag in the impingement zone is normally much stronger than the shear-induced lift.

It is worth noting that the obtained solution may also serve to describe the impingement of a suspension jet on a plane surface, particularly with regard to the effect of particle collisions on surface erosion and heat transfer, e.g. in a rocket exhaust plume or for enhancing heat transfer from a wall (Kitron *et al.* 1989).

4. RESULTS AND DISCUSSION

Simulations of the various flow systems were performed with the time interval Δt_m set equal to the estimated $0.1/\nu$. The flow field must be simulated during about 800 time intervals in order to obtain the steady-state particle distributions. In the absence of gravity, the approach of the particle axial velocity profile to that of the gas served as a useful indication for the approach to the steady state.

The results obtained were particularly interesting with respect to the radial distribution of the particle concentration. The distributions of particle concentrations for pipe flows are presented in figures 2–5.

The low sensitivity of the numerical solution with respect to the number of particles allocated per cell was established by a comparison of solutions obtained for pipe flows with different numbers of cells, which indicated that increasing the number of cells above 10 did not change the concentration distribution patterns significantly.

In laminar flow in a pipe, starting from a uniform radial particle concentration, neglecting the Saffman force and gravity and for uniformly sized particles, a build-up of particle concentration towards the wall and, to a lesser extent, towards the pipe core was observed when inter-particle collisions were taken into account (figure 2).

While lift forces such as the Magnus and Saffman forces could account for the particle drift towards the pipe axis, as explained in section 2.6 above, only a few explanations have been proposed to account for the drift away from the axis. Soo (1969) accounted for the drift away from the axis by employing a particle diffusivity attributed to the perturbation of the flow fields by the particles.

An alternative mechanism for particle diffusivity due to inter-particle collisions can be proposed on the basis of the numerical results. Particles colliding at the pipe core may be deflected towards the wall, where they are slowed by the gas flow near the walls. Due to their small velocities, particles

near the wall collide less frequently and hence are less likely to return to the pipe core. Particles may also lose velocity by colliding with the wall and, consequently, remain near the wall. The latter effect is similar to the deposition of "granular heat" near walls, described by Haff (1983) for the flow of dense granular materials. Furthermore, particles deflected towards the wall may reach a zone where their axial velocity exceeds that of the gas, and will thus be drawn by the Saffman force farther towards the wall.

A weaker effect due to particle collisions is the concentration maximum at the pipe core. This effect may be attributed to the small velocity gradient in the pipe core, causing relatively low particle collision rates. When the Saffman force is taken into account, the lag of particle velocities relative to gas velocities results in an inward force, producing a predominant concentration at the pipe core.

Notably, radial migration of solid particles may be caused by local instabilities in shear flows (see Fichman & Pneuli 1987). A small perturbation in the motion of particles of diameter

$$d > 2.36\left(\frac{\rho_p}{\rho_G}\right)^{-1/3}\left[\left(\frac{\rho_G}{\mu_G}\right)\left(\frac{dU_z}{dr}\right)\right]^{-1/2} \qquad [36]$$

will cause them to migrate with increasing velocity in the direction of the perturbation velocity perpendicular to that of the main flow. Thus, Fichman & Pneuli deduced that particles in regions where the above criterion is met will tend to migrate away from these regions. Thus, in laminar pipe flows the small velocity gradient in the pipe core may be expected to cause particles to concentrate in this region. In the analysed flows, criterion [36] was always met at some locations in the pipe (e.g. for the conditions in figure 2 and at $r = D/4$, $2.36(\rho_p/\rho_G)^{-1/3}[(\rho_G/\mu_G)(dU_z/dr)]^{-1/2} = 0.74d$). Since inter-particle collisions may be regarded as a perturbation of particle velocities, the migration towards the pipe core may be accounted for by the above mechanism. As for the migration towards the pipe wall, one should note that since the collisions rate near the wall is likely to be relatively low (due to small velocities near the wall), perturbations in this region will also be less frequent, so that particle migration away from this zone will also be relatively small.

In the absence of particle collisions, corresponding to the particle volume fraction tending to zero, the particles remain uniformly distributed. Increasing the particle volume fraction to $<1\%$ enhances particle migration towards the wall. A further increase in the particle volume fraction causes a rise in the particle concentration at the pipe core and near the wall, with an additional peak formed at an intermediate zone between the wall and the pipe core (figure 2). The reason for the appearance of this additional peak is apparently the screening effect of high particle concentrations near the wall, preventing particles from reaching the wall.

When gravity was taken into account, in vertical pipe flow with values of the Froude number, $\mathrm{Fr} = U^2/(gD)$, of the order of 10, the radial concentration gradient vanished. The effect of gravity to reduce the radial gradients in vertical pipe laminar flows may be explained on the basis of the above reasoning. When gravity is taken into account, particles in the region adjacent to the wall no longer maintain small velocities. Rather, they soon attain a high downward velocity which can cause them to collide with particles which penetrate into this region and thereby attain a radial velocity, allowing them to migrate back into the pipe core.

Thus, the solutions shown in figure 2 represent limiting cases. The significance of gravity effects in vertical pipe flows may be assessed by combining [20] and [25] above, to obtain the following condition for neglecting gravity effects:

$$\frac{\left(\frac{\rho_G}{\rho_p} - 1\right)\mathrm{Re}_0}{\mathrm{Fr}} \ll 1, \qquad [37]$$

where $\mathrm{Re}_0 = \rho_G d\bar{U}/\mu_G$.

Moreover, neglecting the Saffman force in this case is not justified, since when this force is taken into consideration, an overwhelming migration of particles towards the pipe core is obtained.

Solutions for laminar pipe flows (in the absence of gravity and the Saffman force) indicate that the concentration gradient near the wall increases when increasing either of the following

parameters: the particle Reynolds number Re_0, the ratio between the particle and the pipe diameters, and the solid to gas densities ratio, ρ_p/ρ_G. The dependence of the concentration gradient on these parameters may be examined by expressing the hydrodynamic Knudsen number as

$$S = \tau_h \frac{\bar{U}}{D} = \frac{\left(\frac{\rho_p}{\rho_G}\right) Re_0 \left(\frac{d}{D}\right)}{18}. \qquad [38]$$

Thus, increasing the parameters which increase the concentration maximum near the wall, i.e. ρ_p/ρ_g, Re_0 and d/D, all result in an increase in S; this is because an increase in S indicates a weaker effect of the particle–gas interactions and thus an increase in the effect of inter-particle collisions. Increasing d/D also increases Kn and hence may be expected to exert an ambiguous influence over the concentration maximum; nevertheless, its tendency to increase the concentration maximum appears predominant.

The deviation of the particle collision dynamics from the elastic, frictionless collision model reduces the concentration gradient near the wall. Nevertheless, for deviations of the order of 0.2 in the values of the elasticity and friction parameters (ε, η) from the values corresponding to ideal model of perfect elasticity and no friction, the particle concentrations were virtually the same as for the ideal model. This means that the solution is not strongly sensitive to the collision parameter values, which is important since the values of such parameters are difficult to measure.

Turbulent pipe flows were simulated for Re_0 values above 100 and particle sizes of $d/D = 0.005$ or smaller, so that $Re_D = Re_0 D/d$ was of the order 1×10^5, and thus the assumption of a locally homogeneous and stationary turbulent velocity field was valid. Moreover, as discussed above, for the simulated conditions ($Re_0 \sim 500$, $d/D \sim 0.005$, $\rho_p/\rho_G \sim 1000$) the values of τ_L (see [30]) and τ_h (see [20]) may be calculated as $\tau_L \sim 5D/\bar{U}$ and $\tau_h \sim 100D/\bar{U}$, so that for $\beta \sim 0.001$ [32] indicates a negligible modulation of the gas turbulence intensity caused by the presence of solid particles.

In turbulent pipe flows, for equal size particles with a uniform inlet concentration distribution over the pipe cross-section, a build-up of the particle concentration towards the wall and towards the pipe core was obtained in several cases (figures 3 and 4). This trend was obtained for vertical pipe flow, taking account of gravity and the Saffman force with respect to the average gas velocity shear, both with and without inter-particle collisions.

A migration towards the core, in the absence of inter-particle collisions, has been predicted by considering gas shear-induced forces (Saffman force etc.) acting upon particles (see Yuu 1980). Similarly to the arguments presented in the above discussion of laminar flows, the radial migration towards the pipe wall may be attributed to the "trapping" of particles in the slow-moving laminar gas layer, where no radial gas motion is present. The radial migration may be induced by radial velocities of turbulent eddies, as well as by inter-particle collisions.

The Saffman force did not affect the concentration distribution pattern significantly. Also, unlike the case of laminar pipe flows, the effect of gravity does not prevent the radial migration of particles; this is because in turbulent gas flows Fr values are likely to be larger, due to the high gas velocities. Moreover, in turbulent pipe flows [37] above will be more likely to hold than in laminar flow systems.

Increasing the particle volume fraction to 0.0015 caused an increase in the concentration peak near the wall (figure 3); this indicates that inter-particle collisions intensified the particle migration mechanism described above. A further increase in β to 0.015 resulted in a smaller concentration peak near the wall (figure 3). A plausible explanation is that at high collision rates, the enhanced momentum transfer between particles hinders the formation of large concentration gradients.

As demonstrated in figure 4, an increase in the solid to gas densities ratio ρ_p/ρ_G resulted in an increased concentration maximum at the pipe core and higher particle concentrations close to the wall. Increasing the particle diameter, the particle Reynolds number, Re_0, and the elasticity of inter-particle collisions similarly enhanced these concentration maxima. These effects can all be accounted for, as in laminar flow, by the increase in the hydrodynamic Knudsen number S, [38].

Since, as discussed above, the phenomenological model employed for the turbulent flow field involved several adjustable parameters in the expression for the Lagrangian time scale τ_L, the sensitivity of the model to variations in these parameters was tested by changing the coefficient in

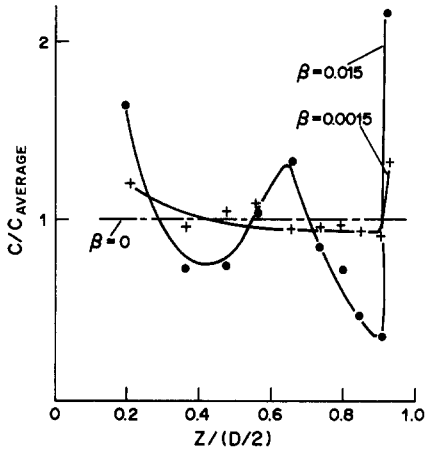

Figure 2. Effect of particle volume fraction on particle radial concentration profiles in laminar flow in a pipe (no gravity or lift forces, $Re_0 = 5$, $d/D = 0.005$, $\rho_p/\rho_G = 1000$, $\varepsilon = 1, \eta = 0, \varepsilon_w = 1, \eta_w = 0$).

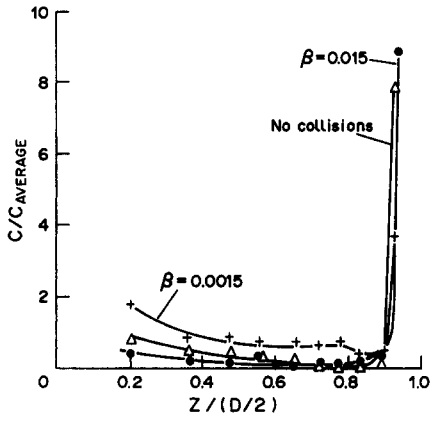

Figure 3. Particle radial concentration profiles in turbulent flow in a vertical pipe, with and without collisoins and for different particle volume fractions ($Re_0 = 500$, $d/D = 0.005$, $\rho_p/\rho_G = 1000$, $\varepsilon = 1, \eta = 0, \varepsilon_w = 1, \eta_w = 0$, Fr = 8000).

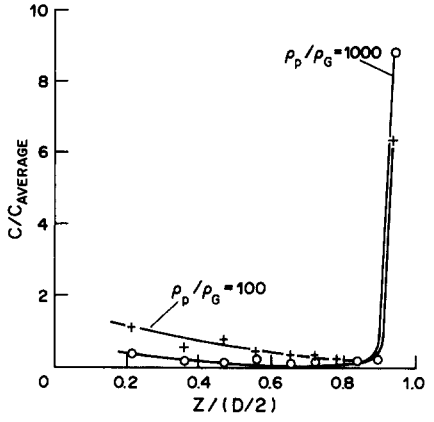

Figure 4. Particle radial concentration profiles in turbulent flow in a vertical pipe, for different particle to gas densities ratios ($Re_0 = 500$, Fr = 8000, $d/D = 0.005$, $\beta = 0.0015$, $\varepsilon = 1$, $\eta = 0$, $\varepsilon_w = 1$, $\eta_w = 0$).

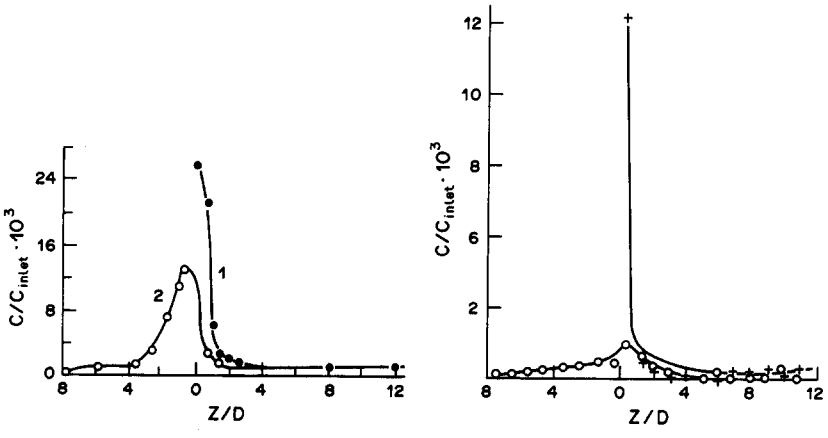

Figure 5. Particle axial concentration profiles along the core ($0 < r < 0.275D$) of an impinging streams reactor. *Left*—experimental results (Elperin 1972); *right*—simulation results, following 800 simulation intervals of duration $0.092L/U_0$ each. [No lift forces or gravity, particle inlet axial velocity = $0.1U_0$, Re_0 (based on velocity U_0) = 1808, $\beta_{inlet} = 6.1 \times 10^{-4}$, $d/L = 0.00337$, $D/L = 0.0714$, $H/D = 0.5$, $\rho_p/\rho_G = 933$, $\varepsilon = 1$, $\eta = 0$, $\varepsilon_w = 1$, $\eta_w = 0$, each side of the reactor divided into 20 axial cells].

[30] for τ_L. Increasing τ_L by a factor of 2 (for $Re_0 = 500$, $d/D = 0.005$, $\rho_p/\rho_G = 1000$, $\beta = 0.0015$) hardly affected the concentration pattern.

To study the validity of the predicted concentration distribution patterns, calculations were made for some turbulent suspension flows for which experimental results have been reported. Lee & Durst (1982) reported that in a vertical turbulent pipe flow of glass particles suspended in air particles tended to migrate towards the pipe core. Numerical simulation for the corresponding flow parameters ($d/D = 0.001$, $\rho_p/\rho_G = 880$, $\beta = 0.00063$, $Re_0 = 80$, $Fr = 80$) yielded concentration maxima both at the pipe core and near its walls. Notably, the numerical results show an increase in the particle concentration towards the core over most of the pipe cross-section, while the concentration maximum near the wall is restricted to a very narrow layer. In vertical turbulent pipe flow, the concentration maximum near the wall might not be detected in experiments because of the enhanced fallout of particle clusters. In Lee's (1987) analysis of the concentration distribution patterns reported by Lee & Durst (1982), the migration towards the core is attributed to lift forces (Saffman force etc.). Nevertheless, in the vicinity of the wall Lee predicts a significant fluid drifting velocity towards the wall, due to the large concentration of particles at the core. The large values of the fluid velocity towards the wall and the large turbulent viscosity cause a considerable increase in the drag force on the solid particles. Particles are thus propelled towards the wall and once they have penetrated a region where their axial velocity exceeds that of the gas they continue to move towards the wall under the action of the Saffman force, which is enhanced by the increase in the fluid's turbulent viscosity. This mechanism may cause migration of large particles towards the pipe wall. While Lee suggests that the radial migration of particles towards the wall is caused by the change in the turbulent viscosity in two-phase suspension flows, the results obtained in this work allow us to explain the same phenomenon by considering direct interactions between particles.

In simulations of turbulent pipe flows of mixtures of particles of different size or density, the concentration gradients for the particles were generally more pronounced than in their single-component flow under identical conditions. Similar patterns were obtained for laminar pipe flows of particle mixtures, in the absence of gravity. The reason for the increased particle migrations is that flows of particle mixtures generally involve higher collision rates than in corresponding single type flows, due to differences in the response to the flow field between particles of different size or density.

In the analysis of the flow in the impinging streams reactor shown in figure 1, the flow parameters used in Elperin's (1972) experiments were employed, while the assuming particle inlet velocities to amount to 10% of the gas velocity. In the absence of gravity, the steady state was not obtained in the simulation, with particles accumulating in the impingement zone; nevertheless, calculations were made in the absence of gravity so as to indicate the net effect of inter-particle collisions. The particle concentration distribution profiles over the reactor core, calculated following 800 time intervals of size $0.092L/U_0$ (so that for $L = 0.3$ m and $U_0 = 30$ m/s, $\Delta t_m = 0.009$ s) are presented in figure 5 for symmetrical and one-sided injections of particles. The results are in qualitative agreement with those reported by Elperin (1972) (see the left-hand part of figure 5); quantitative agreement is not possible due to the omission of gravity effects in the calculation. Results obtained for collisionless flow, aimed at investigating the extent of the effect of collisions on the exiting of particles from the system, display extremely high concentrations in the impingement zone, indicating that collisions considerably reduced the particle concentration in the impingement zone, in agreement with Elperin's (1972) assessment.

The simulation of a one-sided injection of particles demonstrates the penetration of particles from one stream into the other, and the effect of particle collisions due to particle oscillations between the opposite streams. The particle collision rate is higher for a two-sided feed compared to a one-sided feed, resulting in decreased residence times and decreased distance of penetration into the opposite stream.

It must be noted that the build-up of particle concentration in the vicinity of the impingement plane is due to the familiar process of particle accumulation in a zone of flow stagnation. Nevertheless, the penetration of particles from one stream into the other is clearly visible in the case of a one-sided particle feed, and the effects of collisions between particles from opposite streams as well as collisions with particles oscillating between the streams are quite pronounced in the results obtained with the aid of the model presented above.

REFERENCES

ABRAHAMSON, J. 1975 Collision rates of small particles in a vigorously turbulent fluid. *Chem. Engng Sci.* **30,** 1371–1379.

AL-TAWEEL, A. M. & LANDAU, J. 1977 Turbulence modulation in two-phase jets. *Int. J. Multiphase Flow* **3,** 341–351.

BIRD, G. A. 1968 The structure of normal shock waves in a binary gas mixture. *J. Fluid Mech* **31,** 657–668.

BIRD, G. A. 1976 *Molecular Gas Dynamics.* Clarendon Press, Oxford.

BOOTHROYD, R. G. 1971 *Flowing Gas–Solids Suspensions.* Chapman & Hall, London.

CLIFT, R., GRACE, J. R. & WEBER, M. E. 1978 *Bubbles, Drops and Particles.* Academic Press, London.

CULICK, F. E. C. 1964 Boltzmann equation applied to a problem of two phase flow. *Phys. Fluids* **7,** 1894–1904.

ELPERIN, I. T. 1961 Heat and mass transfer in impinging streams. *Inzh.-fiz Zh.* **6,** 62 (in Russian).

ELPERIN, I. T. 1972 *Transport Processes in Impinging Jets.* Nauka i Tekhnika, Minsk (in Russian).

FICHMAN, M. & PNEULI, D. 1987 Migration of solid particles perpendicular to a local shear flow due to local instabilities. *AIAA Jl* **25,** 1016–1018.

HAFF, P. K. 1983 Grain flow as a fluid-mechanical phenomenon. *J. Fluid Mech.* **48,** 477–505.

HETSRONI, G. 1982 *Handbook of Multiphase Systems.* Hemisphere, Washington, D.C.

HINZE, J. O. 1972 Turbulent fluid and particle interaction. *Prog. Heat Mass Transfer* **6,** 433–452.

HINZE, J. O. 1975 *Turbulence.* McGraw-Hill, New York.

JENKINS, J. T. & SAVAGE, S. B. 1983 A theory of the rapid flow of identical, smooth, nearly elastic, spherical particle. *J. Fluid Mech.* **130,** 187–202.

KITRON, A., ELPERIN, T. & TAMIR, A. 1989 Monte Carlo simulation of wall erosion and heat transfer by a gas–solids suspension. *J. Thermophys. Heat Transfer.* **3,** 112–122.

LANGMUIR, I. & BLODGET, K. 1948 Mathematical investigation of water droplet trajectories. *J. Met.* **5,** 175.

LAUFER, J. 1954 The structure of turbulence in fully developed pipe flow. *NASA tech. Note* **1174,** 417–434.

LAWN, C. J. 1971 The determination of the rate of dissipation in turbulent pipe flow. *J. Fluid Mech.* **48,** 477–505.

LEE, S. L. 1982 Aspects of suspension shear flows. *Adv. appl. Mech.* **22,** 1–65.

LEE, S. L. 1987 A unified theory on particle transport in a dilute two-phase suspension flow—II. *Int. J. Multiphase Flow* **13,** 137–144.

LEE, S. L. & DURST, F. 1982 On the motion of particles in turbulent duct flows. *Int. J. Multiphase Flow* **8,** 125–146.

LEE, S. L. & WIESLER, M. A. 1987 Theory of transverse migration of particles in a turbulent two-phase suspension flow due to turbulent diffusion—I. *Int. J. Multiphase Flow* **13,** 99–111.

LIFSHITZ, E. M. & PITAEVSKII, L. P. 1981 *Physical Kinetics.* Pergamon Press, Oxford.

MARBLE, F. E. 1964 Mechanism of particle collision in the one-dimensional dynamics of gas–particle mixtures. *Phys. Fluids* **7,** 1270–1282.

MICHAEL, D. H. & NOREY, P. W. 1969 Particle collision efficiencies for a sphere. *J. Fluid Mech.* **37,** 565–575.

NANBU, K. 1980 Direct simulation scheme derived from the Boltzmann equation. I. Multi-component gases. *J. phys. Soc. Japan* **49,** 2042–2049.

OGAWA, S. 1983 On the statistical approaches to the dynamics of fully fluidized granular materials. In *Advances in the Mechanics and Flow of Granular Materials,* pp. 601–612. Trans-Tech Publications,

OWEN, P. R. 1969 Pneumatic transport. *J. Fluid Mech.* **39,** 407–432.

PAI, S. I. 1974 Fundamental equations of a mixture of a gas and small spherical solid particles from simple kinetic theory. *Revue Roum. Sci. Tech. Mec. Appl.* **19** (4), 605–621.

PEARSON, H. J. VALIOULIS, I. A. & LIST, E. J. 1984 Monte Carlo simulation of coagulation in discrete particle-size distributions. I. Brownian motion and fluid shearing. *J. Fluid Mech.* **143,** 367–385.

PERRY, R. H. & CHILTON, C. H. 1973 *Chemical Engineering Handbook*, 5th edn. McGraw-Hill, Kogakusha, Japan.

SAFFMAN, P. G. 1965 The lift on a small sphere in a slow shear flow. *J. Fluid Mech.* **22,** 385–400. *Idem*, 1968 Corrigendum. *Ibid.* **31,** 624.

SHAHINPOOR, M. & AHMADI, G. 1983 A kinetic theory for the rapid flow of rough inelastic spherical particles and the evolution of fluctuations. In *Advances in the Mechanics and Flow of Granular Materials*, Vol. 2, pp. 641–667. Trans-Tech Publications.

SOO, S. L. 1967 *Fluid Dynamics of Multiphase Systems.* Blaisdell, Waltham, Mass.

SOO, S. L. 1969 Pipe flow of suspensions. *Appl. scient Res.* **21,** 68–84.

SOO, S. L. 1976 Net effect of pressure gradient on a sphere. *Phys. Fluids* **19,** 757.

SOO, S. L. 1983 Dynamic interactions of granular materials. In *Advances in the Mechanics and Flow of Granular Materials*, pp. 675–698. Trans-Tech Publications.

TAMIR, A. & KITRON, A. 1987 Applications of impinging streams reactors. *Chem. Engng Process. Rev.* **50,** 241–330.

VOINOV, O. V. & PETROV, A. G. 1977 The stability of a small body in non-uniform flow. *Soviet Phys. Dokl.*, **22,** 722–724.

YOSHIDA, H. & MASUDA, H. 1980 Model simulation of particle motion in turbulent gas–solid pipe flow. *Powder Technol.* **26,** 217–220.

YUU, S. 1980 Particle concentration distribution in a turbulent stream in a horizontal circular pipe. *Kagaku Kogaku Ranbunshu* **6,** 70–78.